Computers and Chemical Engineering 126 (2019) 249–262

Contents lists available at ScienceDirect

Computers and Chemical Engineering

journal homepage: www.elsevier.com/locate/compchemeng

Global optimization of multicomponent distillation configurations: Global minimization of total cost for multicomponent mixture separations

Zheyu Jiang[a,1], Tony Joseph Mathew[a], Haibo Zhang[a,2], Joshua Huff[a,3], Ulaganathan Nallasivam[a,4], Mohit Tawarmalani[b], Rakesh Agrawal[a,*]

[a] Davidson School of Chemical Engineering, Purdue University, West Lafayette, IN 47907, USA
[b] Krannert School of Management, Purdue University, West Lafayette, IN 47907, USA

ARTICLE INFO

Article history:
Received 23 December 2018
Revised 6 April 2019
Accepted 8 April 2019
Available online 11 April 2019

Keywords:
Multicomponent distillation
Distillation configuration
Global optimization
Cost optimization
Process intensification

ABSTRACT

We introduce a global optimization framework for determining the minimum cost required to distill any ideal or near-ideal multicomponent mixture into its individual constituents using a sequence of columns. This new framework extends the Global Minimization Algorithm (GMA) previously introduced by Nallasivam et al. (2016); and we refer to the new framework as the Global Minimization Algorithm for Cost (GMAC). GMAC guarantees global optimality by formulating a nonlinear program (NLP) for each and every distillation configuration in the search space and solving it using global optimization solvers. The case study presented in this work not only demonstrates the need for developing such an algorithm, but also shows the flexibility and effectiveness of GMAC, which enables process engineers to design and retrofit energy efficient and cost-effective distillation configurations.

1. Introduction

Multicomponent distillation is ubiquitous in chemical and process industries (Humphrey, 1992) and deals with some of worlds largest and most profitable separations, such as crude oil fractionation, hydrocarbon separations from steam cracking, and natural gas liquids (NGL) separations. Multicomponent distillation is generally performed in a sequence of distillation columns known as a distillation configuration. To separate a n-component mixture into n pure products, it has been shown that the group of distillation configurations that use exactly $n-1$ columns are lucrative because they incur minimum operating cost while requiring modest capital investment relative to other groups of configurations that either use less than $n-1$ columns or more than $n-1$ columns (Giridhar and Agrawal, 2010a). We refer to configurations with $n-1$ columns as the regular-column configurations. Regular-column configurations can be further categorized into two types: 1) basic and 2) thermally coupled. A regular-column configuration is called basic if each column has one reboiler and one condenser (Agrawal, 2003). Thermally coupled configurations are derived from basic configurations by replacing one or more submixture heat exchangers (i.e. heat exchangers that do not produce final pure products) with two-way vapor-liquid transfers known as thermal couplings. Unfortunately, selecting the best regular-column configuration remains hard because the number of regular-column configurations increases combinatorially as the number of components in the feed increases (Shah and Agrawal, 2010). Each column in a configuration may perform various splits, where each split separates a mixture into two product streams. A split is called a sharp split if the product streams have no overlapping components, where as it is called a non-sharp split if some of the components in both product streams are the same and are present in amounts that are not negligible. Accordingly, regular-column configurations can be further classified as either sharp split configurations if all their splits are sharp or non-sharp split configurations if at least one of their splits is non-sharp.

Although these distillation configurations perform the same separation task, they can have very different capital and operating costs. Considering this variation, it is valuable to devise techniques that help process engineers identify a configuration or a set of configurations such that the total cost these configurations incur for a given separation task is close to the minimum possible. To

* Corresponding author.
E-mail addresses: mtawarma@purdue.edu (M. Tawarmalani), agrawalr@purdue.edu (R. Agrawal).

[1] Present address: Corteva Agriscience, Midland, MI 48640, USA.
[2] Present address: ExxonMobil Asia Pacific PTE Ltd. 098623, Singapore.
[3] Present address: Marathon Petroleum Corporation, Findlay, OH 45840, USA.
[4] Present address: Yokogawa Electric Corporation, Bangalore 560048, India.

https://doi.org/10.1016/j.compchemeng.2019.04.009
0098-1354/

identify alternative configurations, it is important to first characterize the complete set of regular-column configurations. Towards this end, Sargent and Gaminibandara (1976) proposed a superstructure that includes both sharp and non-sharp split configurations, but this superstructure does not exhaustively cover all regular-column configurations. In particular, Agrawal (1996) discovered a new set of configurations wherein the feed column communicates with all the remaining columns and extended the superstructure to include these configurations. Later, Agrawal (2003) identified a set of rules and proposed a stepwise enumeration procedure to capture the feasible basic and thermally coupled regular-column configurations. Nevertheless, Giridhar and Agrawal (2010b) observed that even the latter method omitted certain configurations when the separation task involves 5 or more components. To address this, they proposed a network formulation based on a set of logical constraints that captured all basic regular-column configurations. Finally, Shah and Agrawal (2010) developed a simple and elegant six-step method to systematically generate the complete search space of all basic and thermally coupled regular-column configurations with sharp and/or non-sharp splits. Here onwards, we refer to the method of Shah and Agrawal (2010) as the SA method.

Because the number of regular-column configurations increases rapidly with the number of components in the feed (Giridhar and Agrawal, 2010b), it is too inefficient and expensive to use process simulators, such as Aspen Plus, to perform rigorous simulations for each and every configuration in the search space so as to identify an attractive configuration. Instead, researchers are interested in formulating an optimization problem that considers all configurations in the search space and identifies a few lucrative alternatives. Caballero and Grossmann (2001) developed a superstructure based on a state-task network representation for thermally coupled configurations, including the completely thermally coupled (CTC) ones in which all submixture heat exchangers are replaced with thermal couplings. Their superstructure was modeled as a generalized disjunctive program. Subsequently, Caballero and Grossmann (2004) extended their earlier superstructure to capture all basic and thermally coupled regular-column configurations. The authors then solved the resulting generalized disjunctive program as a mixed-integer nonlinear program (MINLP) in order to identify the configuration that minimizes the total cost. However, the MINLP could not be solved to global optimality and the local nonlinear programming (NLP) solver failed to give a feasible solution due to singularity issues that arose due to column sections that disappear (Caballero and Grossmann, 2001). The procedure was computationally expensive and even if a solution was found, it was often a poor local optimum. Therefore, Caballero and Grossmann (2001) proposed an algorithm by modifying the logic-based outer-approximation algorithm. Nevertheless, they were still unable to guarantee global optimality with this approach (Caballero and Grossmann, 2001).

Caballero and Grossmann (2004) then proposed a two-step iterative optimization procedure to solve the MINLP. In the first step, they focused on identifying the best CTC configuration, while the second step was to determine the best locations where thermal couplings could be replaced with heat exchangers. They have extended this solution procedure to consider heat integration (Caballero and Grossmann, 2006), column section rearrangements (Caballero and Grossmann, 2003), and dividing wall columns (Caballero and Grossmann, 2013). In short, this two-step iterative procedure decomposes the original problem, such that instead of simultaneously finding the optimal topological structure and the optimal submixture heat exchangers placement, these are done sequentially. Since it is not necessary that the configuration with minimum total cost corresponds to a CTC configuration which is the least costly among all CTC configurations, this decomposition is not guaranteed to find the true optimal solution for the original optimization problem.

The cost model of Caballero and Grossmann (2004) makes several simplifying assumptions that may affect the choice of the optimal configuration. For example, a fixed capital cost of $150,000 is assumed for all reboilers and condensers (Franco and Grossmann, 2014), whereas, in practice, the cost of heat exchanger depends on various factors including its type and the actual heating or cooling duty requirement. Also, contrary to practice, in their model, the number of stages in a distillation column does not depend on the column's reflux ratio. Instead, the model computes the minimum number of stages using the Fenske equation (Fenske, 1932) and sets the number of stages to be twice of this minimum. Furthermore, in their model, all condensers, including the ones at submixtures, can only produce saturated liquid streams. Such condensers at submixtures may result in an unnecessarily large penalty in energy requirement and the total cost at submixtures. In summary, these simplifications and modeling assumptions do not correctly account for the capital and energy costs and tend to underestimate the former while overestimating the latter thereby eschewing the choice of distillation configurations towards potentially less desirable configurations.

Besides the above simplifying assumptions, the model of Caballero and Grossmann (2004) is incomplete in how it computes the minimum vapor duty requirement of a distillation column using Underwood's method (Underwood, 1948). The current constraints admit solutions that are physically infeasible and thus underestimate the actual vapor duty requirement. Although the MINLP formulation and the two-step iterative procedure of Caballero and Grossmann (2004) made significant advances to the state of the art, a model that addresses these deficiencies will be able to more closely approximate the total cost and thus more accurately identify configurations that incur less total cost. A number of MILP or MINLP formulations based on detailed tray-by-tray calculations have also been developed in the literature, some of which consider special applications such as homogeneous azeotropic distillation (Kraemer et al., 2009), heterogeneous azeotropic distillation (Skiborowski et al., 2015), dividing wall columns (Waltermann and Skiborowski, 2017), etc. However, due to model complexity, most of these studies focus on separations involving no more than four component mixtures and their models can only be solved to local optimality.

Apart from the MINLP based approach discussed above, a different approach to identify the optimal distillation configuration is to first enumerate the complete search space, and then to formulate an optimization problem for each configuration to decide how to build and operate that configuration with the lowest possible cost. Nallasivam et al. (2016) recently adopted this enumeration based approach and proposed an algorithm that solved an NLP problem to minimize the total reboiler vapor duty requirement for every basic and thermally coupled regular-column configuration in the search space. The configurations were enumerated using the SA method (Shah and Agrawal, 2010) and each NLP was solved to global optimality using BARON (Tawarmalani and Sahinidis, 2005). This algorithm was called Global Minimization Algorithm (GMA), and is the first algorithm to guarantee global optimality for minimizing vapor duty. Although GMA requires significant computational effort because it solves an NLP for every individual configuration in the search space, it is amenable to parallelization. In addition, a number of strategies such as bound tightening (Nallasivam et al., 2016) can be used to reduce the computational time substantially. In this article, we extend the GMA approach by developing a general NLP based formulation that minimizes the total cost of any regular-column distillation configuration. This general formulation is referred to as the Global Minimization Algorithm for Cost, or simply **GMAC** for short.

The total cost of a distillation configuration comprises of two parts: the capital cost and the operating cost. The capital cost of a configuration depends on various attributes such as the number and sizes of distillation columns, trays, reboilers, and condensers. Assuming that all reboilers use the same heating utility and all condensers use the same cooling utility, the operating costs associated with these heat exchangers are directly proportional to the vapor duty generated/condensed at the heat exchanger. Also, considering the operating life of the facility, the annual interest rate as well as inflation must be incorporated into the overall cost. All these factors will be captured in the GMAC formulation. In the formulation presented in this paper, the majority of the GMA framework is retained and modifications are made to incorporate additional cost related relations. We will present these equations in the next section. The strategies and techniques used to improve convergence and reduce computational time for each NLP problem are elucidated in Nallasivam et al. (2016).

In Section 3, we study a five-component alcohol mixture separation example to demonstrate the usefulness and robustness of the GMAC approach. We will then compare our results with the solution obtained using the two-step iterative procedure. Finally, we vary various parameters and discuss how the optimal solutions change. These analyses illustrate that our GMAC approach is flexible and will allow process designers to not only design new attractive distillation systems, but also retrofit existing ones.

2. NLP formulation

Any optimization problem is described by the decision variables, the objective function, and the constraints. The GMAC formulation retains all the decision variables and most of the constraints from the GMA framework described in Nallasivam et al. (2016). The objective in GMAC is to minimize the total annualized cost TAC which is defined as a weighted sum of the fixed capital investment FCI and the yearly operating cost YOC:

$$\min \quad \mathrm{TAC} = k_{\mathrm{FCI}}\mathrm{FCI} + k_{\mathrm{YOC}}\mathrm{YOC}, \tag{1}$$

where the coefficients k_{FCI} and k_{YOC} are nonnegative constants provided by the user. For example, if a user is interested in finding configurations that are cheap to build, then k_{FCI} is set to be 1 and k_{YOC} is set as 0 to minimize the capital cost. Conversely, if operating cost is the primary concern, the user can specify $k_{\mathrm{FCI}} = 0$ and $k_{\mathrm{YOC}} = 1$. When both capital and operating costs need to be considered, it is common to use the total annualized cost as the objective function (Turton et al., 2012), in which $k_{\mathrm{YOC}} = 1$ and FCI is annualized by assuming certain payback or depreciation period L (typically 8–10 years) and estimating an annual interest rate r as well as an annual inflation rate f. The effective interest rate r', after accounting for inflation, is thus given by $\frac{r-f}{1+f}$ (Turton et al., 2012). With this, the coefficient k_{FCI} for total annualized cost estimation is determined as the inverse of the annuity factor:

$$k_{\mathrm{FCI}} = \frac{r'(1+r')^L}{(1+r')^L - 1} \tag{2}$$

A feasible distillation column operation must satisfy vapor-liquid equilibrium and appropriate mass balance relations. In addition, the vapor flow requirement for carrying out a given separation in a distillation column section satisfies Underwood's equations (Underwood, 1948), which employ the underlying assumptions of ideal liquid-vapor equilibrium, constant relative volatility, and constant molar overflow. The full set of constraints implied by these relationships has been thoroughly discussed in Nallasivam et al. (2016) and is retained in the formulation proposed here with one exception. In practice, the optimal operation of a distillation column is usually achieved between 1.1 and 1.5 times its minimum reflux ratio (Sundaram and Evans, 1993). Using the heuristic that the actual reflux ratio is 20% higher than the minimum reflux ratio, we have, for each and every split s, $L_s^{\mathrm{top}} \geq 1.2L_s^{\min} = 1.2(V_s^{\min} - \sum_{k=i}^{n-j+i} \overline{X}_{s,k})$. This eventually leads to:

$$\begin{aligned} V_s^{\mathrm{top}} \geq\ & 1.2V_s^{\min} \\ & -0.2\sum_{k=i}^{n-j+i} \overline{X}_{s,k} \qquad i = \mathrm{ROW}(\mathrm{DISTS_s}); \\ & \qquad\qquad j = \mathrm{COL}(\mathrm{DISTS_s});\ \forall s = 1, \ldots, n_s \end{aligned} \tag{3}$$

where as described in Nallasivam et al. (2016), V_s^{top} is the actual vapor flow in the upper column section of split s, $V_s^{\min}$ is the minimum upper section vapor flow determined by Underwood's distillate constraint (Underwood, 1948), $\overline{X}_{s,k}$ stands for the net material upward flow in the upper section of split s. The quantity DISTS_s gives the stream number associated with the split's top product as discussed in Nallasivam et al. (2016). A stream number labels a material stream based on the components it contains in non-negligible quantities. For example, stream AB denotes a material stream composed of components A and B. Here, A, B, C, and so on represent pure components with their volatilities decreasing in alphabetical order. Based on the definitions of Shah and Agrawal (2010) and Nallasivam et al. (2016), $\mathrm{ROW}(m)$ corresponds to the lightest component number in material stream m, and $\mathrm{COL}(m)$ is equal to the number of components present in stream m. For instance, when $m = \mathrm{BCD}$, $\mathrm{ROW}(m) = 2$ which stands for the second most volatile component (i.e. component B), and $\mathrm{COL}(m) = 3$. Finally, n_s denotes the number of splits present in the configuration.

We need to point out that the minimum vapor duty constraints used to calculate $V_s^{\min}$ for each split s, which are published in the articles describing the MINLP (Caballero and Grossmann, 2004; 2006) and NLP algorithms (Nallasivam et al., 2016), have not been formulated correctly. Instead of allowing them to be inequality constraints, Underwood's distillate constraints (Underwood, 1948) must be introduced as an equalities with respect to the active Underwood roots associated with split s, which are related to the key components of the split (Halvorsen and Skogestad, 2003):

$$\begin{aligned} V_s^{\min} = & \sum_{k=i}^{n-j+i} \frac{\alpha_k \overline{X}_{s,k}}{\alpha_k - \theta_{s,r}} \quad \forall r = \text{active root};\ i = \mathrm{ROW}(\mathrm{DISTS_s}); \\ & j = \mathrm{COL}(\mathrm{DISTS_s});\ \forall s = 1, \ldots, n_s \end{aligned} \tag{4}$$

Note that only the active Underwood roots $\theta_{s,r}$ associated with split s are selected in Eq. (4). A discussion on how to select the active Underwood roots can be found in Tumbalam Gooty et al. (2018). If Underwood's distillate constraints are introduced as inequalities instead, the system would have too much flexibility than it should have. This can possibly lead to physically infeasible solution of $\overline{X}_{s,k}$ when performing the vapor duty calculations based on Underwood's method (Tumbalam Gooty et al., 2018). We believe that Caballero and Grossmann (2004) did not implement Equation (4) as the formulation is available in Franco and Grossmann (2014). Nallasivam et al. (2016) also did not describe these equalities, even though they did implement them in their computations, including all the case studies presented in their work.

As mentioned before, the main modification to the model of Nallasivam et al. (2016) is that we introduce cost relations to GMAC, which we describe now. The FCI is estimated by the total module cost C_{TM} which can be approximated by the product of the total purchase costs of major pieces of process equipment in the facility and the appropriate Lang factor

F_{lang} (Lang, 1947; Turton et al., 2012):

$$\text{FCI} \approx C_{\text{TM}} = F_{\text{lang}} k_{\text{CEPCI}} \left(\sum_{c \in \text{REB}} C_{\text{reb},c} + \sum_{c \in \text{COND}} C_{\text{cond},c} + \sum_{s=1}^{n_s} C_{\text{col},s} + \sum_{s=1}^{n_s} C_{\text{tray},s} \right) \tag{5}$$

in which $C_{\text{col},s}$, $C_{\text{tray},s}$, $C_{\text{reb},c}$, and $C_{\text{cond},c}$ are purchased equipment costs associated with the column shell that carries out split s, tray stages in the column associated with split s, reboiler at column c, and condenser at column c, respectively. Here, sets reb and cond are sets of distillation column indices in a configuration that have a reboiler and condenser associated with them, respectively. Fluid processing plants typically have a Lang factor of 4.74 (Turton et al., 2012). The multiplier k_{CEPCI} is the ratio of Chemical Engineering Plant Cost Index (CEPCI) (Vatavuk, 2002) between the present time and the time when the capital cost correlations are tabulated. It accounts for the increase of purchased equipment costs due to inflation.

Next, we specify the cost correlations used in Eq. (5). For a distillation column c, the tray cost $C_{\text{tray},c}$ depends on the type of tray used, the diameter (A_c) of the column, and the number of tray stages (N_c) in the column. Such correlations have been tabulated in several references including Turton et al. (2012) for various tray types. These correlations are expressed as second-order polynomials with respect to A_c:

$$C_{\text{tray},c} = N_c(k_{\text{tray},0} + k_{\text{tray},1} A_c + k_{\text{tray},2} A_c^2) \tag{6}$$

where $k_{\text{tray},0}, k_{\text{tray},1}, k_{\text{tray},2}$ are constants specified by the users based on the actual implementation. The total number of trays N_c in distillation column c can be estimated using a variety of methods. One of them is to first use the Fenske–Underwood–Gilliland method to estimate the number of trays associated with each split s in column c. These estimates are then added together to obtain the number of stages in the distillation column. Eduljee (1975) offers the following alternative form to the Gilliland's correlation (Gilliland, 1940):

$$\frac{N_s - N_{s,\min}}{N_s + 1} = 0.75 \left[1 - \left(\frac{R_s - R_{s,\min}}{R_s + 1} \right)^{0.5688} \right], \tag{7}$$

where N_s is expressed as a function of the minimum number of stages ($N_{s,\min}$), the minimum reflux ratio ($R_{s,\min}$), and the actual reflux ratio R_s. $N_{s,\min}$ is determined using the Fenske equation (Fenske, 1932) and R_s is chosen to be $1.2R_{s,\min}$. As we can readily see, Eq. (7) is highly nonlinear and nonconvex. To avoid introducing more nonlinearity and nonconvexity into the optimization model, Caballero and Grossmann (2013) simply replaced the right hand side (RHS) of Eq. (7) with a constant. This constant was derived by evaluating the RHS for a range value of $R_{s,\min}$. These values were chosen based on typical operating conditions for various distillation columns. And such substitution was justified based on the observation that the RHS is relatively insensitive to $R_{s,\min}$ in this range. Or, one could also use a simple power law fit in terms of $R_{s,\min}$ to approximate the RHS of Eq. (7). In our GMAC formulation, users have the flexibility to choose the equation form for the RHS as they desire, based on their expected range of operating reflux ratios of distillation columns. Using the fact that the left hand side (LHS) of Eq. (7) is a monotonically increasing function of N_s, while the RHS is a monotonically decreasing function of $R_{s,\min}$ when substituting $R_s = 1.2R_{s,\min}$, one can easily show that the value of N_s is respectively lower and upper bounded by $\frac{4 \cdot 6^a}{6^a+3} N_{s,\min} + \frac{3(6^a-1)}{6^a+3}$ and $4N_{s,\min} + 3$, where $a = 0.5668$. Knowing these bounds on decision variables can tighten the GMAC formulation and foster convergence.

For split s, the minimum number of stages $N_{s,\min}$ is calculated a priori using the Fenske equation (Fenske, 1932) by pre-specifying the fractional recovery β of the light key in the distillate and the fractional recovery δ of the heavy key in the bottoms product:

$$N_{s,\min} = \frac{\ln\left(\frac{\beta\delta}{(1-\beta)(1-\delta)} \right)}{\ln \alpha} \qquad \forall s = 1, \ldots, n_s, \tag{8}$$

in which α is the relative volatility ratio of the light key and heavy key associated with split s. A light key/heavy key of split s is defined as the lightest/heaviest component that distributes, or would distribute between the top and bottom products if the vapor duty in split s decreases by infinitesimal amount (Halvorsen and Skogestad, 2003).

The cross sectional area $A_{\text{col},s}$ of a column section is calculated for each split s using the equation from Doherty and Malone (2001):

$$A_{\text{col},s} = \frac{M_{\text{av}}}{\sqrt{\rho_v \rho_l}} \frac{k}{\phi_{\text{flood}} c_0} \max\{V_s^{\text{top}}, V_s^{\text{bot}}\} \qquad \forall s = 1, \ldots, n_s \tag{9}$$

where M_{av} is the average molecular weight of the components in the system, ρ_v and ρ_l are respectively the mass density of liquid and vapor present on the tray, ϕ_{flood} is the fraction of flooding velocity desired in the design, typically between 0.6 and 0.75, and c_0 is a constant in Fair's correlation (Fair, 1987) that is related to the tray spacing. For a tray spacing of 24 in. (61 cm), c_0 is estimated as 439 m/h (Doherty and Malone, 2001). The coefficient k stands for the inverse of the fraction of total cross sectional area available for flow. A typical value for k is $1/0.8 = 1.25$. Finally, V_s^{top} and V_s^{bot} are the vapor flows in the upper and lower column sections associated with split s, respectively. These constants and coefficients are all user-defined parameters in the NLP formulation.

As we have previously mentioned, for a non-sharp split configuration, at least one distillation column contains more than one split. For such a distillation column, the column shell cost and tray cost can be estimated in one of the two ways. In the first option, the column diameter of column split section is determined by Eq. (9) and then the split is connected to neighboring column sections using converging or diverging cone sections. Such cone sections add height and cost to the column. In the second option, the column shell has a uniform diameter and adjustments are made to the open areas in various tray sections so that the column can be operated properly. This option increases column diameter in certain sections, which adds cost. Generally, when designing a distillation column with multiple feeds and side-draws, a process designer uses both these methods and, to minimize costs, certain sections are connected through cone sections while other sections adjust internally. Currently, we do not have an easy method at our disposal to calculate the costs associated with different cone sections. Therefore, we assume the column shell has a uniform diameter which is the maximum among all splits in the column. Therefore, we appropriately modify Eq. (9) into:

$$A_{\text{col},c} \geq \frac{M_{\text{av}}}{\sqrt{\rho_v \rho_l}} \frac{k}{\phi_{\text{flood}} c_0} \max\{V_s^{\text{top}}, V_s^{\text{bot}}\} \quad \forall c = 1, \ldots, n-1,\ s \in \text{COLS}_c \tag{10}$$

where the set COLS_c gives the split indices associated with distillation column c. The overall height (H_c) of distillation column shell c is related to the total number of trays within the column as well as extra spacings that account for 1) the liquid sump at the bottom of the column, 2) the surge capacity and vapor disengaging space at the top (Doherty and Malone, 2001), and 3) necessary height for liquid collectors and redistributors, especially when the column involves multiple splits. We lump these contributors together and denote this extra spacing for split s as h_s. Thus, H_c can be written as:

$$H_c = \sum_{s \in \mathrm{COLS}_c} k_H N_s + h_s \qquad \forall c = 1, \ldots, n-1 \tag{11}$$

where k_H is the desired tray spacing specified by the users, typically between 0.3 m and 0.6 m.

Once $A_{\mathrm{col},c}$ and H_c have been defined, we express the purchase cost ($C_{\mathrm{col},c}$) of the column shell associated with column c as:

$$C_{\mathrm{col},c} = k_{\mathrm{col},0} + k_{\mathrm{col},1} A_{\mathrm{col},c} H_c \qquad \forall c = 1, \ldots, n-1 \tag{12}$$

The reboiler and condenser costs ($C_{\mathrm{reb},c}$ and $C_{\mathrm{cond},c}$) for column c depend on the type of heat exchanger used, the type of construction material, and the heat transfer area. The heat transfer area is related to the overall heat transfer coefficient of the heat exchanger and its approach temperature. Again, these parameters are pre-specified to the GMAC model. Assuming that the distillation system operates at or near ambient pressure so that no special material is required, we can formulate the heat exchanger cost as a linear function of heat transfer area:

$$\begin{aligned} C_{\mathrm{reb},c} &= k_{\mathrm{reb},0} + k_{\mathrm{reb},1} A_{\mathrm{reb},c} && \forall c \in \mathrm{REB} \\ C_{\mathrm{cond},c} &= k_{\mathrm{cond},0} + k_{\mathrm{cond},1} A_{\mathrm{cond},c} && \forall c \in \mathrm{COND} \end{aligned} \tag{13}$$

As we have pointed out earlier, if the capital cost for heat exchangers in a distillation configuration is assumed to be fixed, the total annualized cost TAC in Eq. (1) may underestimate FCI and recommend configurations with more heat exchangers. Typically, this results in an unduly large penalty for thermally coupled configurations which have lower energy need and thus a smaller YOC. It is thus not suitable to fix the capital cost of a heat exchanger if it is to be estimated accurately. Instead, this cost should depend on various factors discussed above and, in particular, the heat transfer area. The heat transfer area $A_{\mathrm{reb},c}(A_{\mathrm{cond},c})$ associated with reboiler(condenser) for column c can be estimated from the heat transfer rate Q using the overall heat transfer coefficient U and the log mean temperature difference (LMTD). U and LMTD are parameters specified by the user. We assume, for simplicity of presentation, that LMTD is the same for all reboilers and condensers, U_{reb} is the same for all reboilers, and U_{cond} is the same for all condensers. Then, $A_{\mathrm{reb},c}$ and $A_{\mathrm{cond},c}$ are given as follows:

$$\begin{aligned} A_{\mathrm{reb},c} &= \frac{Q_{\mathrm{reb},c}}{U_{\mathrm{reb}}\mathrm{LMTD}} = \frac{V_s^{\mathrm{bot}}}{U_{\mathrm{reb}}\mathrm{LMTD}} \frac{\sum_{k=i}^{n-j-i}(X_{m,k}\Delta H_k)}{\sum_{k=i}^{n-j-i} X_{m,k}} \\ &\quad \forall c \in \mathrm{REB},\ s \in \mathrm{SBOT}_c,\ m = \mathrm{BOTTS}_s, \\ &\quad i = \mathrm{ROW}(m),\ j = \mathrm{COL}(m) \\ A_{\mathrm{cond},c} &= \frac{Q_{\mathrm{cond},c}}{U_{\mathrm{cond}}\mathrm{LMTD}} = \frac{V_s^{\mathrm{top}} - V_m}{U_{\mathrm{cond}}\mathrm{LMTD}} \frac{\sum_{k=i}^{n-j-i}(X_{m,k}\Delta H_k)}{\sum_{k=i}^{n-j-i} X_{m,k}} \\ &\quad \forall c \in \mathrm{COND},\ s \in \mathrm{STOP}_c,\ m = DISTS_s, \\ &\quad i = \mathrm{ROW}(m),\ j = \mathrm{COL}(m), \end{aligned} \tag{14}$$

where ΔH_k is the molar latent heat of vaporization for component k. The elements in the sets $\mathrm{SBOT_c}$ and $STOP_{\mathrm{c}}$ correspond to the splits respectively located at the bottom and top of distillation column c. Looking back at Eq. (14), it is clear that the term $\sum_{k=i}^{n-j-i}(X_{m,k}\Delta H_k)/\sum_{k=i}^{n-j-i} X_{m,k}$ gives the average molar latent heat of vaporization for stream m, assuming that the interaction between any two components in the mixture is negligible.

This completes the discussion of the equations and correlations used to estimate FCI. We now estimate the YOC of a distillation configuration based on the cost of manufacturing (COM), which is expressed as a weighted combination of the utility costs (C_{ut}) and the fixed capital investment (FCI). The latter accounts for the maintenance of equipment, the supplies, depreciation, administration costs, local taxes and insurances, etc. (Anderson, 2009; Douglas, 1988; Turton et al., 2012). Then, YOC is expression as:

$$\begin{aligned} YOC \approx \mathrm{COM} &= k_{\mathrm{COM},0}\mathrm{FCI} + k_{\mathrm{COM},1}C_{\mathrm{ut}} \\ &= k_{\mathrm{COM},0}\mathrm{FCI} + k_{\mathrm{COM},1}\left(\sum_{c \in \mathrm{REB}} C_{\mathrm{ut,reb,c}} + \sum_{c \in \mathrm{COND}} C_{\mathrm{ut,cond,c}}\right), \end{aligned} \tag{15}$$

where $k_{\mathrm{COM},0}$ is estimated to be 0.28 when the annual depreciation of FCI is 10%, whereas $k_{\mathrm{COM},1}$ is chosen to be 1.23 (Turton et al., 2012). The utility cost associated with reboiler or condenser i is simply given by:

$$\begin{aligned} C_{\mathrm{ut,reb,c}} &= Q_{\mathrm{reb},c} \times \mathrm{OpHr} \times C_{\mathrm{heat}} && \forall c \in \mathrm{REB} \\ C_{\mathrm{ut,cond,c}} &= Q_{\mathrm{cond},c} \times \mathrm{OpHr} \times C_{\mathrm{cool}} && \forall c \in \mathrm{COND} \end{aligned} \tag{16}$$

where $Q_{\mathrm{reb},c}$ and $Q_{\mathrm{cond},c}$ are respectively the heat duty supplied by the reboiler and removed by the condenser for column c, OpHr denotes the operating hours in one year (typically around 8000 h), and C_{heat} and C_{cool} represent unit heating and cooling utility cost, respectively. Again, as a first estimate, we assume that the heating/cooling utilities used in all reboilers/condensers have similar costs. With this, the optimization model formulation for the GMAC is now finalized. Compared to the GMA framework, the GMAC formulation contains additional decision variables that are needed for the cost model, including $A_{\mathrm{col},c}$, N_s, $Q_{\mathrm{reb},c}$ and $Q_{\mathrm{cond},c}$ as defined earlier. In summary, the cost model used in the GMAC framework differs from that of Caballero and Grossmann (2004) in the following major ways:

1. Corrections have been made to Underwood's distillate constraint to accurately determine the minimum vapor duty required for a split.
2. Reboiler and condenser capital costs are no longer fixed. Instead, the cost of a heat exchanger is now a function of the total heat transfer area required, which is proportional to the vapor duty generated or condensed in the heat exchanger.
3. Rather than fixing the total number of trays in a distillate column to be exactly twice the minimum number of trays, users can flexibly choose among various correlations such as that given by Eduljee (1975).
4. For a distillation column consisting of multiple splits, instead of using individual column diameters for each split without accounting for cone costs, a uniform column diameter which is the maximum among all splits is used for the entire column.

The NLP problem for every configuration synthesized using the SA method (Shah and Agrawal, 2010) is solved in GAMS using the global optimization solver BARON (Tawarmalani and Sahinidis, 2005). In the next section, we will consider a specific case study in detail to illustrate the reliability and robustness of GMAC.

3. Case study – alcohols separation

We consider a five-component atmospheric pressure distillation example studied in Caballero and Grossmann (2004, 2006) that concerns with the separation of a five-component mixture of alcohols: ethanol (component A), isopropanol (B), 1-propanol (C), isobutanol (D), and 1-butanol (E). The relative volatilities of these components with respect to the heaviest component E are determined from Poling et al. (2001) as $\{\alpha_A, \alpha_B, \alpha_C, \alpha_D, \alpha_E\} = \{4.1, 3.6, 2.1, 1.42, 1.0\}$, indicating that these separations are relatively difficult to perform (Barnicki and Fair, 1990). The main feed is a saturated liquid stream whose component flow rates are given by $\{f_A, f_B, f_C, f_D, f_E\} = \{20, 20, 80, 60, 20\}$ kmol/h. The latent heats of vaporization for these components are estimated to be $\{\Delta H_A, \Delta H_B, \Delta H_C, \Delta H_D, \Delta H_E\} = \{38.80, 39.41, 41.62, 46.37, 45.41\}$ MJ/kmol.

Table 1
Cost related parameters for GMAC in the Scenario 1.

Cost parameters	Unit	Value
Annual interest rate r	%	9
Annual inflation rate f	%	2.5
Operating life L	year	10
k_{CEPCI} between the year 2017 and 2001	–	535.3/397 = 1.348
$k_{\text{tray},0}, k_{\text{tray},1}, k_{\text{tray},2}$ for sieve tray	\$, \$/m^2, \$/m^4	555.9, 411.12, 22.138
Fractional recovery of light key/heavy key component	–	0.98/0.99
Average liquid and vapor density ρ_l, ρ_v	kg/m^3	723.9, 2.63
ϕ_{flood} of Eq. (10)	–	0.7
c_0 of Eq. (10)	m/h	439
Inverse of free area fraction k of Eq. (10)	–	1.25
Tray spacing k_H, extra spacing h_s for each split s	m	0.6, 4
$k_{\text{col},0}, k_{\text{col},1}$	\$, \$/m^3	4373.5, 672.28
$k_{\text{reb},0}(k_{\text{cond},0}), k_{\text{reb},1}(k_{\text{cond},1})$	\$, \$/m^2	18538, 60.173
U_{reb} and U_{cond} for fixed-tube exchangers	W/Km^2	800
LMTD across heat exchangers	K	10
$k_{\text{COM},0}, k_{\text{COM},1}$ in Eq. (15)	–	0.28, 1.23
Yearly operating hours YOC	h	8000
Cost of low pressure steam C_{heat}	\$/GJ	2
Cost of cooling water C_{cool}	\$/GJ	0.12

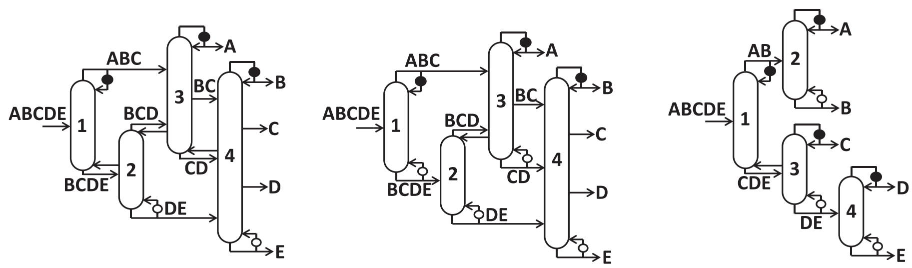

Fig. 1. (a) The optimal configuration with the lowest TAC among all 6128 configurations under Scenario 1; (b) a second configuration that has the same topological structure as the configuration of (a) but with only one thermal coupling. It is among the top 1% in terms of TAC of all 6128 configurations; (c) the best sharp split configuration in terms of minimum TAC that has a ranking of 4685 out of 6128 configurations.

3.1. Scenario 1 – minimizing total annualized cost

Scenario 1 minimizes the combined annualized capital cost and operating cost, i.e. the TAC of a distillation configuration. Under this scenario, we use the cost parameters listed in Table 1. We formulate a general NLP problem for each of the 6128 distillation configurations in MATLAB and solve each NLP problem in GAMS using the BARON solver (Tawarmalani and Sahinidis, 2005) by connecting MATLAB and GAMS using the GAMS/MATLAB interface (Ferris et al., 2011). All 6128 configurations are solved to global optimality ($\leq 1\%$ duality gap) within 4.91 hours of CPU time using a Dell OptiPlex 5040 desktop. We utilize all four of its Intel Quad-Core i7-6700 processors using the Parallel Computing Toolbox in MATLAB.

Among all 6128 flowsheets, the configuration with the lowest total annualized cost of 1.691 million USD (in 2017's value) is shown in Fig. 1a. Table 2 shows the main results and optimal operating conditions for this configuration. We mention that the GMAC approach generates a ranklist of distillation configurations based on their minimum total annualized cost. This ranklist is useful when a process designer has considerations in addition to total cost, because it allows the practitioner to identify a few attractive candidates with similar total annualized costs and make detailed comparisons, among which may be analysis of which configurations are easier to build and/or to operate. For example, the configuration of Fig. 1b, which is among the top 1% of all 6128 configurations in terms of minimum TAC (1.745 million USD), has the same topological structure as the optimal configuration of Fig. 1a but uses two more reboilers at submixtures *BCDE* and *CD*. These additional reboilers offer potential opportunities for heat integration with other process units in the plant, exploiting which could lead to a further reduction in total cost. Furthermore, the presence of submixture reboilers increases the thermodynamic efficiency of the distillation process, as part of the heat duty originally completely supplied by reboilers at *DE* and *E* as shown in Fig. 1a can now be generated by these submixture reboilers, which operate at less extreme temperature levels.

For a long time, design engineers have been used to designing and building sharp split configurations for most industrial separations. Despite their structural simplicity, sharp split configurations are known to require higher energy compared to non-sharp split ones (Giridhar and Agrawal, 2010b). In this example, the best sharp split configuration in terms of minimum total annualized cost among all basic or thermally coupled sharp split configurations is explicitly drawn in Fig. 1c. This configuration, which has a minimum TAC of 2.405 million USD, which is 42.2% more "expensive" to build and operate than the globally optimal configuration and is ranked 4685th out of all 6128 configurations. Albeit sharp split configurations use the least number of column sections (i.e. $2(n-1)$ for an n-component separation task), they generally consume significantly more heat duty than non-sharp split counterparts. The excess energy requirement translates into larger distillation columns and bigger heat exchangers, both of which increase TAC.

Before moving on to Scenario 2, we would like to emphasize that, while the backbone of GMAC is inherited from the previously developed GMA framework (Nallasivam et al., 2016), they are two independent global optimization algorithms serving two distinct objectives. For a given configuration, the optimal design and operating conditions determined by GMA based on minimizing its reboiler vapor duty will generally be very different from those

Table 2
Main results for the configuration of Fig. 1a under Scenario 1 of minimizing TAC.

Split	Section	Vapor flow (kmol/h)	Liquid flow (kmol/h)
$ABCDE \rightarrow ABC/BCDE$	Rec	177.05	119.88
	Strip	177.05	319.88
$BCDE \rightarrow BCD/DE$	Rec	221.91	140.60
	Strip	398.97	460.48
$ABC \rightarrow A/BC$	Rec	382.18	362.18
	Strip	325.01	362.18
$BCD \rightarrow BC/CD$	Rec	325.01	295.37
	Strip	103.09	154.77
$BC \rightarrow B/C$	Rec	132.24	112.24
	Strip	132.24	179.05
$CD \rightarrow C/D$	Rec	132.24	99.05
	Strip	235.34	253.82
$DE \rightarrow D/E$	Rec	235.34	193.82
	Strip	235.34	255.34
Distillation column	Number of trays	Cross sectional area (m^2)	Q_{reb}/Q_{cond} (kW)
1	5	1.06	-/1332
2	12	2.39	5104/-
3	77	2.29	-/4119
4	60	1.43	2969/1448

determined by GMAC which correspond to its minimum TAC. To illustrate this, we implement Eq. (3) in GMA such that it now finds the operating condition corresponding to the minimum reboiler vapor duty required for a configuration to be operated at 20% above the minimum reflux. Next, we directly evaluate TAC of the configuration at this operating condition and compare the result with the minimum TAC obtained from GMAC. For example, using GMA operating condition at which 2.1% less reboiler vapor duty compared to GMAC vapor duty is required, TAC of the configuration of Fig. 1a is evaluated to be 1.971 million USD, which is 13.0% higher than the minimum TAC obtained from GMAC. Moreover, this configuration now stands at 130th position in the ranklist containing all 6128 regular-column configurations based on TAC directly evaluated at their corresponding GMA operating conditions. As we can see, for a given configuration, the distribution of vapor and liquid flows across different distillation columns affects its TAC significantly. On the other hand, the ranking of the sharp split configuration of Fig. 1c, which we know is 4685 out of 6128 under GMAC, now moves to 337 in the new ranklist based on GMA operating conditions, which will make this configuration mistakenly appear to be an attractive candidate to build. In summary, when it comes to cost minimization, it is not enough to simply use GMA results to evaluate TAC directly. Instead, a new and independent global optimization algorithm such as GMAC is required to fulfill this objective.

3.2. Scenario 2 – minimizing capital cost

In industrial practices, there are circumstances where engineers wish to identify distillation flowsheets that require the least capital investment. For example, in a highly integrated chemical complex where the multicomponent distillation system is just a part of the plant, the operating costs of distillation columns may not be the primary concern of process engineers since excess heating and cooling utilities may be available from other parts of the plant, rendering the operation of the distillation system practically for free. Moreover, the energy price and associated concern varies from time to time and from place to place. For example, the recent shale gas boom has caused the energy prices in the US to drop significantly over the past decade. As mentioned previously, to minimize the annualized capital cost of a distillation configuration using GMAC, one can set k_{YOC} in the objective function of Eq. (1) to 0. For the alcohols separation case treated in Section 3.1, using the

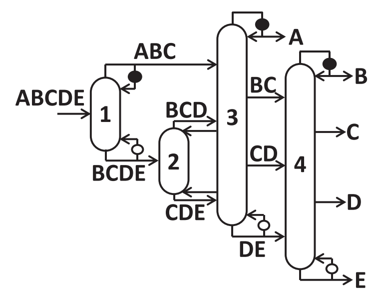

Fig. 2. The optimal configuration with lowest annualized capital cost among all 6128 configurations.

same cost parameters listed in Table 1, we depict, in Fig. 2, the optimal configuration with the lowest minimum annualized capital cost (1.078 million USD, in 2017's value). Surprisingly, it turns out that the second best configuration based on capital cost is the configuration shown in Fig. 1a which minimizes TAC as detailed in Scenario 1. This configuration has a minimum annualized capital cost of 1.088 million USD, which is only 1% higher than the globally optimal solution of Fig. 2. Furthermore, these two configurations are structurally similar. The major difference is that column 2 performs the $BCDE \rightarrow BCD/CDE$ split, whereas column 2 in Fig. 1a performs the $BCDE \rightarrow BCD/DE$ split. This difference causes column 3 in Fig. 2 to have two additional column sections compared to the configuration of Fig. 1a and subsequently leads the presence of an additional split of $CDE \rightarrow CD/DE$.

Just by visually inspecting these two configurations, one might tend to think that the structurally more complex configuration of Fig. 2 should have a higher capital cost than the configuration of Fig. 1a. So why is this configuration cheaper to build? To answer this question, we need to examine the internal vapor and liquid flows inside these distillation columns in both configurations to see how the column sizes and costs are affected accordingly. From Tables 3 and 4, we realize that columns 2 and 4 of Fig. 2 have much smaller column diameters compared to columns 2 and 4 of Fig. 1a, respectively. Consequently, the increase in the cost of column shell for column 3 for the configuration depicted in Fig. 2 is small relative to the decreased costs of column shells for columns 2 and 4. The reason why columns 2 and 4 in the configuration of Fig. 1a have larger diameters is primarily because of the presence of thermal couplings at submixtures *BCDE* and *CD*. In this

Table 3
Main results for the best performing configuration of Fig. 2 under Scenario 2.

Split	Section	Vapor flow (kmol/h)	Liquid flow (kmol/h)
ABCDE → *ABC*/*BCDE*	Rec	209.77	167.37
	Strip	209.77	367.37
BCDE → *BCD*/*CDE*	Rec	230.72	144.26
	Strip	230.72	301.86
ABC → *A*/*BC*	Rec	355.59	335.59
	Strip	313.19	335.59
BCD → *BC*/*CD*	Rec	313.19	257.67
	Strip	82.47	113.42
CDE → *CD*/*DE*	Rec	82.47	57.39
	Strip	313.19	359.26
BC → *B*/*C*	Rec	150.89	130.89
	Strip	150.89	208.80
CD → *C*/*D*	Rec	150.89	128.80
	Strip	150.89	184.83
DE → *D*/*E*	Rec	150.89	124.83
	Strip	150.89	170.89
Distillation column	Number of trays	Cross sectional area (m^2)	Column shell cost (× 1000$)
1	7	1.26	17.03
2	7	1.38	17.75
3	92	2.13	209.26
4	62	0.92	66.74

Table 4
Main results for the second best configuration of Fig. 1a under Scenario 2.

Split	Section	Vapor flow (kmol/h)	Liquid flow (kmol/h)
ABCDE → *ABC*/*BCDE*	Rec	191.65	141.07
	Strip	191.65	341.07
BCDE → *BCD*/*DE*	Rec	217.70	131.82
	Strip	409.35	472.89
ABC → *A*/*BC*	Rec	370.00	350.00
	Strip	319.42	350.00
BCD → *BC*/*CD*	Rec	319.42	283.69
	Strip	101.73	151.87
BC → *B*/*C*	Rec	131.40	111.40
	Strip	131.40	177.71
CD → *C*/*D*	Rec	131.40	97.71
	Strip	233.13	249.58
DE → *D*/*E*	Rec	233.13	189.58
	Strip	233.13	253.13
Distillation column	Number of trays	Cross sectional area (m^2)	Column shell cost (× 1000$)
1	6	1.15	14.46
2	13	2.45	41.33
3	76	2.22	178.62
4	61	1.42	100.34

case, the vapor duty required for *ABCDE* → *ABC*/*BCDE* split in column 1 is completely generated by the reboiler of column 2 before it is transferred to column 1 using the thermal coupling at *BCDE*. Therefore, the internal vapor flow in the stripping section of column 2 (409.35 kmol/h) is significantly more than what is needed for the separation of *BCDE* → *BCD*/*DE*. This increases the diameter of column 2 considerably. Instead, in the configuration of Fig. 2, the internal vapor traffic inside column 2 is 230.72 kmol/h, which results in a much smaller diameter for this column. Similarly, in the configuration of Fig. 1a, part of the vapor duty required for column 3 is supplied by the reboiler of column 4 via thermal coupling at submixture *CD*. This greatly increases the vapor traffic in the lower part of column 4 (233.13 kmol/h) compared to its upper part (131.40 kmol/h), again causing the column to have a larger diameter. For the same reason, even though the configuration of Fig. 2 requires 12 more trays, the overall tray cost $\sum_{c=1}^{4} C_{\mathrm{tray},c}$ of this configuration ($ 499.9k) is still lower than that of Fig. 1a ($ 513.3k). It is worthwhile to revisit our earlier discussion regarding the use of cone sections when diameters for various splits within a column are quite different. Since column 4 in Fig. 1a is a tall column and the difference in the vapor duty below and above the *CD* feed point is quite large, it may be more cost-effective to use a cone to connect the upper and lower sections of the column rather than maintaining an uniform diameter. Another point to note is that in our cost model, we have ignored the liquid/vapor redistributor costs between various column sections. If these were taken into account, configurations such as the one of Fig. 1a would be more favorable because of the fewer column sections relative to the one in Fig. 2. As the cost correlations for these redistributors become available, they can easily be incorporated in the GMAC formulation if needed.

Fig. 3 plots the optimal minimum capital costs for all 6128 configurations in the search space along with their corresponding overall reboiler vapor duty requirements. The overall reboiler vapor duty requirement of a distillation configuration, which is the sum of vapor duties generated at all reboilers, has commonly been used as an indicator of its operating cost (Nallasivam et al., 2016). As a result, industrial practitioners may find such a plot useful in designing energy efficient and cost-effective multicomponent distillation systems. For example, the green box in Fig. 3 contains a

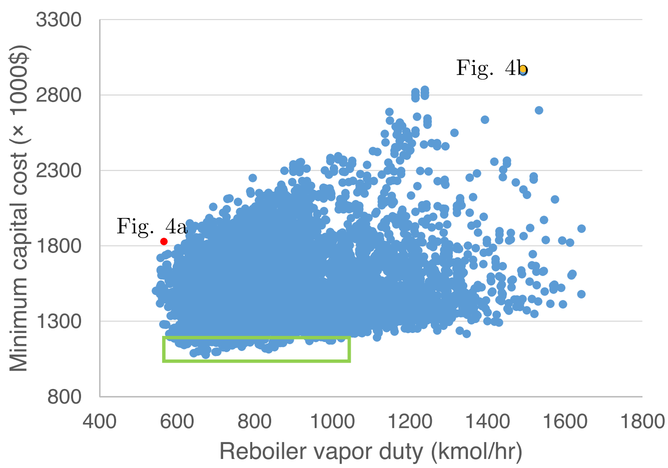

Fig. 3. A plot showing the optimal objective function values (minimum capital cost) and their corresponding total reboiler vapor duty requirements for all 6128 configurations in the search space under Scenario 2. Each dot represents a configuration. The red and yellow dots in the plot corresponds to the configurations of Fig. 4a and b, respectively. (For interpretation of the references to color in this figure legend, the reader is referred to the web version of this article.)

total of 113 configurations that are potentially useful since they require less than 10% higher capital investment compared to the best performing configuration in the search space. These 113 configurations belong to 34 distinct configuration “families”. A configuration “family” is defined as a group of distillation configurations having the same topological structure but the submixtures differ in whether a heat exchanger or a thermal coupling is associated with them. Process engineers have a variety of flowsheet design options to choose from based on factors such as maximum number of thermal couplings, layout of the facility, requirement on the presence and/or absence of certain splits/submixture streams (which is important for retrofitting), etc. Also, note that these 113 configurations cover a wide range of overall reboiler vapor duty requirements. Depending on the actual plant design, some of these configurations with higher total vapor duties might be more attractive than others since they provide heat integration opportunities for reboilers and condensers with other process units in the plant.

Two example configurations are highlighted as the red and yellow dots in Fig. 3 and are explicitly drawn in Fig. 4a and b, respectively. The configuration of Fig. 4a turns out to be the fully thermally coupled (FTC) configuration where the sidedraw streams *BCD, BC*, and *CD* are withdrawn as liquid-only streams. Although it yields the lowest total reboiler vapor duty requirement among all configurations in the search space, the FTC configuration requires the maximum possible number of column sections (i.e. $n(n-1)$ for n-component separation) and submixture streams (i.e. $(n-2)(n+1)/2$), making it expensive to build and difficult to operate (Jiang and Agrawal, 2018; Jiang et al., 2018). From Fig. 3, we see that the configuration of Fig. 4 has a minimum capital cost of 1.828 million USD, which is 69.7% higher than that of the globally optimal solution. Fortunately, one can almost always find at least one non-FTC configuration which consumes almost the same lowest reboiler vapor duty but is much cheaper to build. In this case, we identify 60 additional configurations that would require less than 5% higher total reboiler vapor duty compared to the configuration of Fig. 4a but incur lower capital costs. The best performing configuration among these has a minimum annualized capital cost of 1.186 million USD. This result, when combined with the earlier finding that the FTC configuration is not close to optimality in terms of TAC, demonstrates that building the FTC configuration with its conventional column arrangement is often not a reasonable first choice for a given separation task.

Next, we analyze the example configuration of Fig. 4b which has the highest minimum capital cost compared to all other configurations and a relatively high reboiler vapor duty requirement. This configuration resembles the indirect split configuration except that column 3 performs a non-sharp split, $ABC \rightarrow AB/BC$, making column 4 a two-feed distillation column. Since the main feed enters column 1 as a saturated liquid stream, a large quantity of vapor duty is required to boil all components but *E* to vapor state so that stream *ABCD* can be produced at the top of column 1. This not only increases the capital and operating costs of reboiler at *E*, but also significantly increases the diameters of column 1 as well as all subsequent distillation columns due to the presence of thermal couplings at submixtures *ABCD, ABC*, and *AB*. In addition, these sharp splits in the configuration substantially increase the number of trays required to achieve the desired separations. As a result, the column shells are extraordinarily large and so are the trays. In fact, the annualized capital costs attributed to trays and column shells are respectively 1.522 and 1.046 million USD, more than twice of the corresponding average costs of 0.727 and 0.508 million USD of all 6128 configurations.

One interesting observation regarding the ranklist in Scenario 2 is that sharp split configurations could achieve much higher rankings compared that in Scenario 1. For example, the best performing sharp split configuration, which turns out to be the basic configuration version of Fig. 1c (i.e. thermal coupling at submixture *CDE* is replaced with a reboiler), has a minimum annualized capital cost

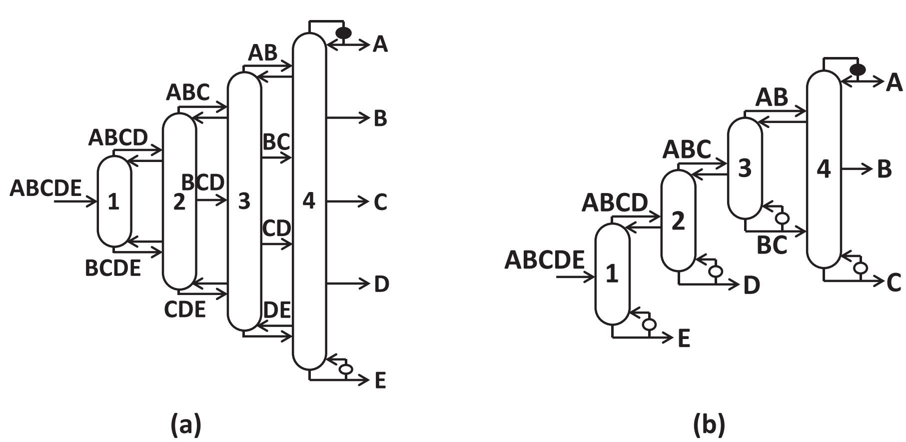

Fig. 4. (a) Example configuration highlighted as red dot in Fig. 3; (b) example configuration highlighted as yellow in Fig. 3. (For interpretation of the references to color in this figure legend, the reader is referred to the web version of this article.)

of 1.217 million USD. Thus, in Scenario 2, it is ranked 252nd out of 6128 configurations in the search space (top 4.1%). In contrast, in Scenario 1, this sharp split configurations was placed at the 4685th position out of all 6128 configurations. Therefore, it is important for industrial practitioners to have a clear idea of their needs and possible plant-wise energy balances so that they can choose the most suitable objective function to use.

4. Ensuring global optimality

As we have discussed, the NLP based GMAC framework guarantees global optimality for each configuration using the global solver BARON (Tawarmalani and Sahinidis, 2005). To compare against the two-step iterative optimization procedure introduced by Caballero and Grossmann (2004), we use the GMAC framework in the following manner that mimics this two-step procedure. This is referred to as the two-step minimization algorithm (TMA). Observe that we still use the more accurate cost correlations and vapor duty calculations in the TMA. In the first step of the iterative procedure of Caballero and Grossmann (2004), all binary variables associated with submixture reboilers and condensers are set to zero, indicating the absence of submixture heat exchangers. Equivalently, in the TMA, only CTC configurations are considered during the first stage. All CTC configurations are optimized in the GMAC framework to ranklist them with respect to their optimal objective function values. In the second step of the iterative procedure of Caballero and Grossmann (2004), the topological structure (i.e. intercolumn connectivity) is fixed to that of the top CTC configuration in the ranklist, whereas the binary variables associated with submixture heat exchangers now become decision variables. This subproblem solves for the optimal arrangement of submixture reboilers and condensers, and the optimal solution from this second step is recorded. In the equivalent TMA approach, all basic and partially thermally coupled configurations belonging to the same family of the top CTC configuration are identified using the SA method and solved to global optimality in the GMAC framework, and the best optimal objective function value among the family of configurations is recorded. Next, the second-best CTC configuration is selected from the ranklist generated at the first step. Then, for its topological structure, heat exchangers are optimally placed at the submixtures. If the newly identified configuration has a lower total cost than the one identified earlier, we examine the third-best CTC configuration on the ranklist of the first step. This process is repeated iteratively until the optimal solution obtained from the second step is worse than the solution determined from the configuration at the previous iteration. The best configuration found by the TMA, which is obtained at the iteration before the last one, is then returned as the best configuration. A process flow chart illustrating the TMA method is shown in Fig. 5. We will compare this configuration with the globally optimal configuration found using GMAC on the complete search space.

In Scenario 1 of the alcohols separation example, the optimal configuration is the one with the lowest minimum total annualized cost. Recall that Fig. 1a illustrates the optimal configuration among all 6128 configurations synthesized by the SA method (Shah and Agrawal, 2010). The TMA terminates with the same configuration. For various case studies we examined, when the payback period is relatively long (8 to 10 years or more), the optimal configuration returned by the TMA method is among the few best configurations returned by the GMAC approach used on the complete search space. This is primarily because, as the payback period gets longer, the contribution of the annualized fixed capital investment FCI to the objective function of Eq. (1) becomes smaller because k_{FCI} reduces with an increase in the payback period L as shown in Eq. (2). Therefore, configurations with lower YOC (in other words, total vapor duty requirement) also tend to have lower minimum

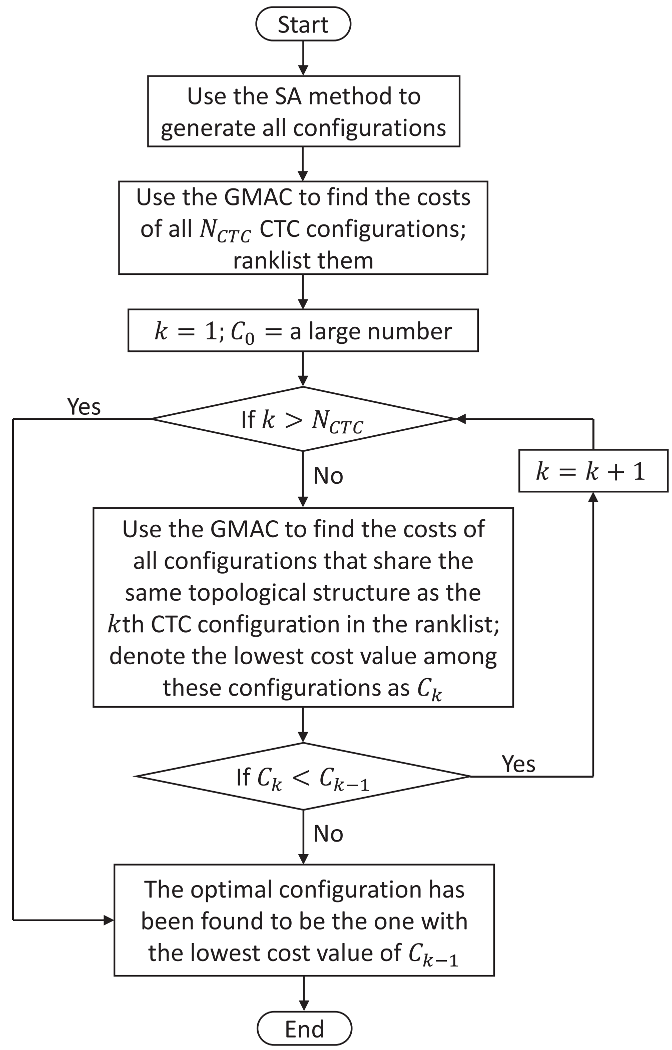

Fig. 5. Process flow chart that simulates the TMA process using the GMAC approach.

TAC compared to those configurations that have higher YOC. As expected, the CTC configuration ranklist obtained during the first step of the TMA matches well with the actual ranklist of configurations obtained in the second step. Thus, the globally optimal configuration often belongs to the configuration family containing the best CTC configuration. In summary, the two-step iterative procedure of Caballero and Grossmann (2004) works quite well for minimizing TAC, when the payback period is long.

On the other hand, in Scenario 2 of the example, where the objective is to minimize the capital cost, or if the payback period is short, the two-step iterative procedure no longer finds the correct globally optimal configuration. This is because the YOC contribution to the objective function now becomes small compared to the FCI contribution. Thus, the CTC configuration ranklist obtained during the first step of the TMA does not match well with the actual ranklist of configurations obtained in the second step. To see this, we use the TMA approach, as shown in Fig. 5, to ranklist the configurations on the basis of minimizing capital cost alone, similar to our Scenario 2. The green dots in Fig. 6 represent the minimum annualized capital costs corresponding to the top 23 CTC configurations identified in Step 1 of the TMA method. And the blue bars represents the lowest minimum capital costs obtained in Step 2 corresponding to the best heat exchanger arrangements. Each iteration stands for a configuration family. The true global op-

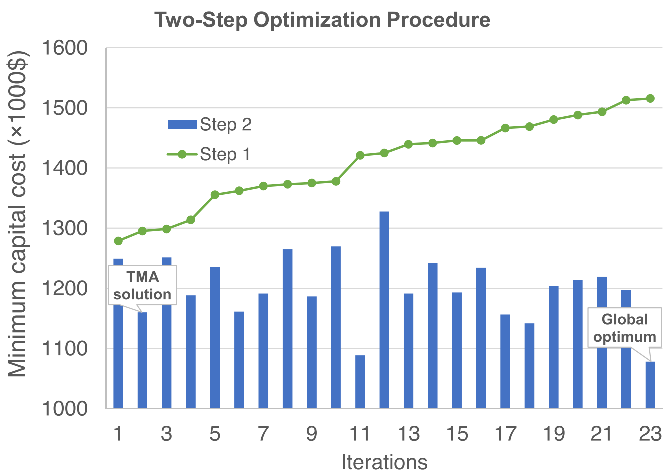

Fig. 6. Results obtained from the two-step optimization procedure (TMA) for Scenario 2. Following the steps shown in Fig. 5, the TMA process would have terminated at the third iteration, even though the true globally optimal solution actually corresponds to the 23rd iteration.

timum as confirmed by GMAC belongs to the 23rd best CTC configuration family and has a minimum capital cost of 1.078 million USD as mentioned before. However, based on the stopping criterion of Caballero and Grossmann (2004), the TMA process would terminate after the first three iterations. It will conclude that the configuration identified in Step 2 of the 2nd iteration, which has a minimum capital cost of 1.160 million USD, is the optimal solution. However, this claim would not be correct. In total, there are 49 configurations with a lower minimum capital cost than that identified by the TMA method. Many of these configurations are attractive candidates from an industrial perspective. This example shows that the two-step iterative procedure proposed by Caballero and Grossmann (2004) does not always give the optimal or near-optimal solution.

Surprisingly, we find out that by simply changing Step 1 from ranklisting all CTC configurations to ranklisting all basic configurations, the globally optimal configuration of Fig. 2 is correctly identified by the TMA method so modified. After examining several case studies, we conclude that, when the objective is to minimize capital costs, this modified TMA approach is more suitable than the proposed approach by Caballero and Grossmann (2004). It is also a reasonable heuristic for cases where the payback period is short. Of course, this approach may still fail to find even a near-optimal solution particularly when the contribution of capital cost is of a magnitude similar to that of the operating cost. Nevertheless, in all cases, one can rely on the GMAC approach to identify the best performing configuration or to generate an accurate ranklist of configurations.

5. Further exploration of process intensification opportunities

For a given multicomponent separation task, our GMAC framework gives the ranklist of all basic and thermally coupled regular-column configurations synthesized by the SA method (Shah and Agrawal, 2010) based on their minimum capital and operating costs. Despite these achievements, one may wonder if there are ways to further reduce the capital and/or operating costs of a distillation configuration.

Recent advances in process intensification (PI) in multicomponent distillation offer interesting directions. Jiang and Agrawal (2018) recently introduced the first systematic, multilayered approach to conduct PI in multicomponent distillation starting from any basic regular-column configuration. Compared to the original configuration, the newly synthesized highly intensified configurations, such as the heat and mass integrated configurations and dividing wall columns, are much more compact, easy-to-operate, energy efficient, and cost-effective. In this section, we will demonstrate some of the PI opportunities that can make the configurations identified by GMAC for the alcohols separation example more compact and cost-effective.

In Scenario 1 of the alcohols separations example, we identify using GMAC that the configuration drawn in Fig. 7a is the one with the least number of column sections among all configurations within whose TAC is within 1% of optimal. This configuration, whose minimum total annualized cost is 1.777 million USD, has two non-sharp splits ($ABCDE \rightarrow ABC/CDE$ and $CDE \rightarrow CD/DE$) and uses only 12 column sections. In this configuration, submixture streams *BC* and *CD* connect column 2 and column 3 respectively with column 4 using a thermal coupling. Column 4 then draws the common component *C* as a final product. One can further reduce the TAC of this configuration and enhance its operability by first converting both thermal couplings of *BC* and *CD* into Agrawal's liquid transfer streams (Agrawal, 2000) and, thereby, eliminate the intercolumn vapor transfer stream. This can be followed by performing a simultaneous heat and mass integration that consolidates columns 2 and 3 into a single column shell of column 2–3 and produces the common final product *C* as a sidedraw stream (Shenvi et al., 2013). The resulting intensified configuration is shown in Fig. 7b. Compared with the original configuration of Fig. 7a, this new configuration uses only three column shells and is thermodynamically equivalent to the original configuration (Jiang and Agrawal, 2018; Shenvi et al., 2013). Thus, despite having to introduce an additional column section to the consolidated column 2–3, the configuration of Fig. 7b is likely to have an

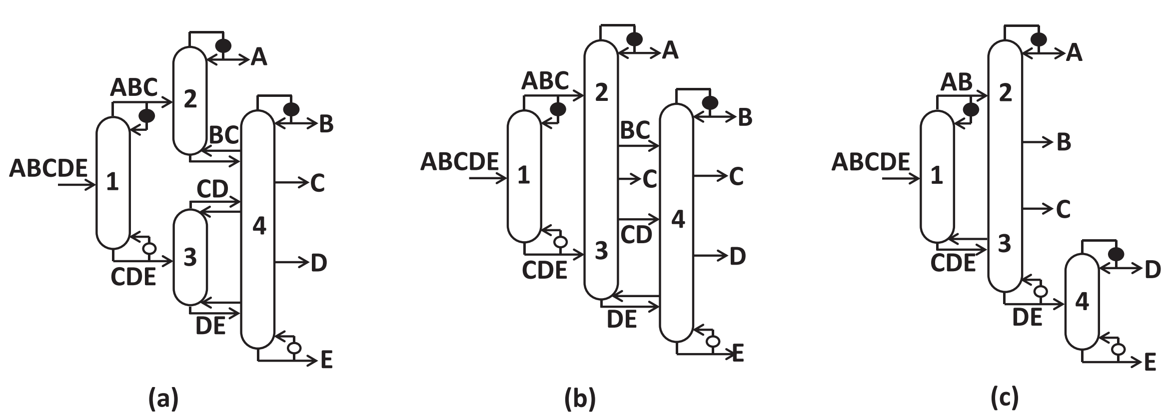

Fig. 7. (a) The configuration within the top 1% of TAC that uses the lowest number of column sections (12 sections); (b) an intensified, more operable configuration derived from (a) following the strategy of Shenvi et al. (2013); (c) a heat and mass integrated configuration derived from Fig. 1c.

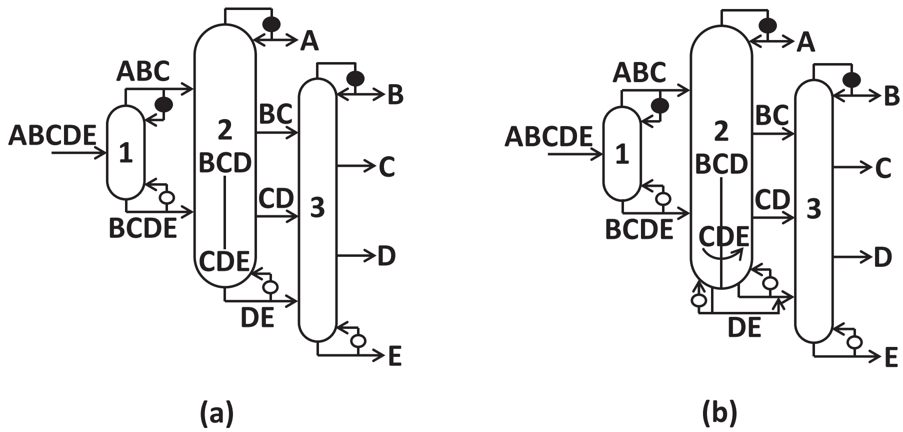

Fig. 8. (a) A thermodynamically equivalent version of Fig. 2 by consolidating columns 2 and 3 into one column shell with a vertical partition. This dividing wall column arrangement is expected to have a lower capital cost compared to that of Fig. 2; (b) an equivalent, operable version of (a) derived by following the methodologies of Madenoor Ramapriya et al. (2018). Submixture *CDE* is now transferred from one zone in the dividing wall column to the other as a liquid-only stream.

even lower TAC compared to the original configuration of Fig. 7a. Besides potentially being more cost-effective, this new configuration also resolves the operability issue associated with thermally coupled columns 3 and 4 in Fig. 7a by converting submixtures *BC* and *CD* into liquid-only streams (Agrawal and Fidkowski, 1998).

Likewise, consider the best performing sharp split configuration drawn in Fig. 1c. We can modify this configuration into the one in Fig. 7c by performing heat and mass integration between a lighter pure product reboiler and a heavier pure product condenser (Jiang et al., 2018). The heat and mass integrated configuration is derived from the original sharp split configuration by eliminating both the reboiler associated with the final product *B* and condenser associated with the final product *C*. This is followed by consolidating columns 2 and 3 into one single column 2–3 while withdrawing pure products *B* and *C* as sidedraws. Of course, the strategy of heat and mass integration can also take place between the reboiler at *B* and the condenser at *D*. However, one can easily verify that the integration between the reboiler at *B* and the condenser at *C* offers greater heat duty savings and thus potentially saves more in heat exchanger costs. Overall, by simultaneously eliminating two heat exchangers and one column shell, we believe that the heat and mass integrated configuration of Fig. 7c can offer substantial reductions in capital and operating costs compared to the original sharp split configuration of Fig. 1c.

Recall that for Scenario 2, Fig. 2 shows the optimal configuration for the alcohols separation example. We recognize that columns 2 and 3 in the optimal configuration of Fig. 2 are especially suited for PI using a dividing wall column (DWC). Compared to conventional distillation configurations, DWCs have been known to substantially reduce the capital cost and the land requirement since they use fewer column shells and other equipment pieces (Agrawal, 2001; Caballero and Grossmann, 2013). For example, as much as 30% capital cost reduction for ternary separations was reported when DWCs were used in place of conventional sharp split configurations (Schultz et al., 2002). For the configuration of Fig. 2, vapor duty generated by the reboiler at *DE* is first split into two fractions, one continues to travel upward within column 3 while the other goes to column 2 through the thermal coupling at *CDE*. These two fractions of vapor traffic will eventually merge back to column 3 above the thermal coupling at *BCD*. It is thus expected that when columns 2 and 3 of Fig. 2 are consolidated into a single column shell with a vertical partition as shown in Fig. 8a, the resulting DWC will have a similar diameter and height as the original column 3. As a result, we have essentially eliminated column 2 from the configuration in Fig. 2 without any significant penalty while saving the costs in column shells. Moreover, the new configuration of Fig. 8a is thermodynamically equivalent to the original regular-column configuration (Madenoor Ramapriya et al., 2018). Therefore, the heat exchanger costs and duties are unlikely to change noticeably after PI. Of course, there is an added cost of the vertical partition, as well as additional costs associated with specially designed column internals and trays for the DWC. Nevertheless, we expect that the intensified configuration of Fig. 8a will perform better than its original regular-column configuration in terms of annualized capital investment.

To solve the operability difficulty of the DWC in the intensified configuration of Fig. 8a due to uncontrolled vapor split at the bottom of the vertical partition, Agrawal and collaborators (Agrawal and Madenoor Ramapriya, 2016) proposed an approach using which one can arrive at a thermodynamically equivalent version shown in Fig. 8b. In this version, the submixture *CDE* is transferred from one zone in the DWC to the other externally as a liquid stream. The extended vertical partition and an additional reboiler that produces the same mixture *DE* make this DWC easy to operate and control, as the desired L/V ratio in both zones of the DWC can be reached and maintained precisely. Note that the sum of heat duties generated at both reboilers that produce the same submixture *DE* of Fig. 8b is equal to that generated at the single reboiler at *DE* of Fig. 8a, meaning that the heat exchanger costs for these two configurations should be similar.

As we can see from these illustrations, synergistic use of the powerful global optimization tool such as the GMAC and conceptual design strategies based on PI can lead to the discovery of completely new and highly intensified configuration flowsheets that are compact and inexpensive to build and are also easy to operate. We believe that these techniques open up many great opportunities for industrial practitioners. Of course, to truly identify the globally optimal configuration design, it would be best to include these new and intensified configurations into the search space of attractive and useful configurations and incorporate them into the GMAC framework. This would require various advances. First, it requires a new superstructure formulation like the SA method (Shah and Agrawal, 2010) that systematically enumerates the search space including all process options. Second, new cost correlations are required to accurately estimate the capital and operating costs associated with these new intensified configurations. We will pursue the development of such a superstructure and cost correlations in the future.

6. Conclusion

This paper develops, for the first time, an enumeration based global optimization algorithm, GMAC, for the global minimization of capital and operating costs of regular-column distillation configurations synthesized by the SA method (Shah and Agrawal, 2010) for distillation of an ideal or a near-ideal multicomponent mixture. While GMAC is inherited from the recently developed GMA framework (Nallasivam et al., 2016) that minimizes reboiler vapor duty for any regular column configuration, it is a standalone global optimization algorithm built exclusively for cost minimization. In GMAC, we develop more accurate cost models compared to those existing in the literature that attempt to address similar problems. GMAC is designed to be flexible and allows the use of various user-defined parameters in its cost correlations. GMAC finds configurations that incur minimum cost by enumerating the search space using the SA method (Shah and Agrawal, 2010) and finding the best way to operate and build each configuration using global optimization techniques. As a result, besides locating the minimum cost configuration, GMAC also generates the complete ranklist of configurations placed in a non-decreasing order of cost incurred.

We have evaluated the GMAC model on various separation examples from the literature that involve separation of 4- to 6-component mixtures. And for each separation task, we found that the GMAC method is capable of optimizing all distillation configurations within an overall time that ranges from minutes to hours, depending on the number of components in the feed. In this article, we presented, in detail, a case study involving separation of a mixture of five alcohols. We derived various valuable insights that can help industrial practitioners choose and design energy efficient and cost-effective configurations. We identified various process intensification ideas to further improve the energy requirement, capital cost, as well as operability of the attractive configurations identified using the GMAC approach. These process intensification strategies include heat and mass integration and consolidation of columns using dividing walls (Jiang and Agrawal, 2018). By using GMAC as a screening tool and utilizing the novel process intensification techniques, process engineers can quickly determine a ranklist of a few attractive configurations. Detailed analyses of these designs can then be performed by using process simulators whiling considering integration with the rest of the plant.

We demonstrated that the two-step iterative optimization procedure which decomposes the original problem into two independent subproblems, does not necessarily find globally optimal solutions. The GMAC method is thus the only economic optimization framework available as of now that guarantees global optimality.

Disclaimer

The information, data, or work presented herein was funded in part by an agency of the United States Government. Neither the United States Government nor any agency thereof, nor any of their employees, makes any warranty, express or implied, or assumes any legal liability or responsibility for the accuracy, completeness, or usefulness of any information, apparatus, product, or process disclosed, or represents that its use would not infringe privately owned rights. Reference herein to any specific commercial product, process, or service by trade name, trademark, manufacturer, or otherwise does not necessarily constitute or imply its endorsement, recommendation, or favoring by the United States Government or any agency thereof. The views and opinions of authors expressed herein do not necessarily state or reflect those of the United States Government or any agency thereof.

Acknowledgments

The information, data, or work presented herein was funded in part by the Office of Energy Efficiency and Renewable Energy (EERE), U.S. Department of Energy, under Award number DE-EE0005768. The authors would like to thank both anonymous reviewers for their valuable input and suggestions.

References

Agrawal, R., 1996. Synthesis of distillation column configurations for a multicomponent separation. Ind. Eng. Chem. Res. 35 (4), 1059–1071.
Agrawal, R., 2000. Thermally coupled distillation with reduced number of intercolumn vapor transfers. AIChE J. 46 (11), 2198–2210.
Agrawal, R., 2001. Multicomponent distillation columns with partitions and multiple reboilers and condensers. Ind. Eng. Chem. Res. 40 (20), 4258–4266.
Agrawal, R., 2003. Synthesis of multicomponent distillation column configurations. AIChE J. 49 (2), 379–401.
Agrawal, R., Fidkowski, Z.T., 1998. More operable arrangements of fully thermally coupled distillation columns. AIChE J. 44 (11), 2565–2568.
Agrawal, R., Madenoor Ramapriya, G., 2016. Multicomponent dividing wall columns. US Patent 9504934B2.
Anderson, J., 2009. Determining manufacturing costs.. Chem. Eng. Prog. 105 (12), 27–32.
Barnicki, S.D., Fair, J.R., 1990. Separation system synthesis: a knowledge-based approach. 1. liquid mixture separations. Ind. Eng. Chem. Res. 29 (3), 421–432.
Caballero, J.A., Grossmann, I.E., 2001. Generalized disjunctive programming model for the optimal synthesis of thermally linked distillation columns. Ind. Eng. Chem. Res. 40 (10), 2260–2274.
Caballero, J.A., Grossmann, I.E., 2003. Thermodynamically equivalent configurations for thermally coupled distillation. AIChE J. 49 (11), 2864–2884.
Caballero, J.A., Grossmann, I.E., 2004. Design of distillation sequences: from conventional to fully thermally coupled distillation systems. Comput. Chem. Eng. 28 (11), 2307–2329.
Caballero, J.A., Grossmann, I.E., 2006. Structural considerations and modeling in the synthesis of heat-integrated-thermally coupled distillation sequences. Ind. Eng. Chem. Res. 45 (25), 8454–8474.
Caballero, J.A., Grossmann, I.E., 2013. Synthesis of complex thermally coupled distillation systems including divided wall columns. AIChE J. 59 (4), 1139–1159.
Doherty, M.F., Malone, M.F., 2001. Conceptual design of distillation systems. McGraw-Hill Chemical Engineering Series. McGraw-Hill, Boston.
Douglas, J.M., 1988. Conceptual design of chemical processes. McGraw-Hill Chemical Engineering Series. McGraw-Hill, New York.
Eduljee, H., 1975. Equations replace gilliland plot. Hydrocarb. Process. 54 (9), 120–122.
Fair, J., 1987. Handbook of Separation Process Technology. John Wiley Sons,New York, NY.
Fenske, M.R., 1932. Fractionation of straight-run pennsylvania gasoline. Ind. Eng. Chem. 24 (5), 482–485.
Ferris, M. C., Dirkse, S., Ramakrishnan, J., 2011. Matlab and gams: Interfacing optimization and visualization software (the gdxmrw utilities). http://research.cs.wisc.edu/math-prog/matlab.html.
Franco, R., Grossmann, I. E., 2014. Optimal separation sequences based on thermally coupled distillation. http://newton.cheme.cmu.edu/interfaces/thermaldis/main.html.
Gilliland, E.R., 1940. Multicomponent rectification estimation of the number of theoretical plates as a function of the reflux ratio. Ind. Eng. Chem. 32 (9), 1220–1223.
Giridhar, A., Agrawal, R., 2010a. Synthesis of distillation configurations: I. Characteristics of a good search space. Comput. Chem. Eng. 34 (1), 73–83.
Giridhar, A., Agrawal, R., 2010b. Synthesis of distillation configurations. ii: a search formulation for basic configurations. Comput. Chem. Eng. 34 (1), 84–95.
Halvorsen, I.J., Skogestad, S., 2003. Minimum energy consumption in multicomponent distillation. 1. Vmin diagram for a two-product column. Ind. Eng. Chem. Res. 42 (3), 596–604.
Humphrey, J.L., 1992. Separation technologies: an opportunity for energy savings. Chem. Eng. Prog. 88, 32–42.
Jiang, Z., Agrawal, R., 2018. Process intensification in multicomponent distillation: a review on recent advancements. Accepted by Chem. Eng. Res. Des.
Jiang, Z., Madenoor Ramapriya, G., Tawarmalani, M., Agrawal, R., 2018. Minimum energy of multicomponent distillation systems using minimum additional heat and mass integration sections. AIChE J. 64 (9), 3410–3418.
Kraemer, K., Kossack, S., Marquardt, W., 2009. Efficient optimization-based design of distillation processes for homogeneous azeotropic mixtures. Ind. Eng. Chem. Res. 48 (14), 6749–6764.
Lang, H.J., 1947. Engineering approach to preliminary cost estimates.. Chem. Eng. 54, 117–122.
Madenoor Ramapriya, G., Tawarmalani, M., Agrawal, R., 2018. A systematic method to synthesize all dividing wall columns for n-component separation: part ii. AIChE J. 64 (2), 660–672.
Nallasivam, U., Shah, V.H., Shenvi, A.A., Huff, J., Tawarmalani, M., Agrawal, R., 2016. Global optimization of multicomponent distillation configurations: 2. enumeration based global minimization algorithm. AIChE J. 62 (6), 2071–2086.
Poling, B.E., Prausnitz, J., O'Connell, J., 2001. The Properties of Gases and Liquids, 5th ed. McGraw-Hill, New York.
Sargent, R., Gaminibandara, K., 1976. Optimal design of plate distillation columns. In: Dixon, L. (Ed.), Optimization in Action. Academic Press, New York. Conference on Optimization in Action (1975 : University of Bristol).
Schultz, M.A., Stewart, D.G., Harris, J.M., Rosenblum, S.P., Shakur, M.S., OBrien, D.E., 2002. Reduce costs with dividing-wall columns. Chem. Eng. Prog. 98 (5), 64–71.

Shah, V.H., Agrawal, R., 2010. A matrix method for multicomponent distillation sequences. AlChE J. 56 (7), 1759–1775.
Shenvi, A.A., Shah, V.H., Agrawal, R., 2013. New multicomponent distillation configurations with simultaneous heat and mass integration. AlChE J. 59 (1), 272–282.
Skiborowski, M., Harwardt, A., Marquardt, W., 2015. Efficient optimization-based design for the separation of heterogeneous azeotropic mixtures. Comput. Chem. Eng. 72, 34–51.
Sundaram, S., Evans, L.B., 1993. Shortcut procedure for simulating batch distillation operations. Ind. Eng. Chem. Res. 32 (3), 511–518.
Tawarmalani, M., Sahinidis, N.V., 2005. A polyhedral branch-and-cut approach to global optimization. Math. Program. 103, 225–249.
Tumbalam Gooty, R., Agrawal, R., Tawarmalani, M., 2019. An MINLP formulation for the optimization of multicomponent distillation configurations. Comp. Chem. Eng. 125 (9), 13–30.
Turton, R., Bailie, R.C., Whiting, W.B., Shaeiwitz, J.A., Bhattacharyya, D., 2012. Analysis, synthesis, and design of chemical processes. Prentice-Hall International Series in the Physical and Chemical Engineering Sciences, fourth ed. Prentice Hall, Upper Saddle River, NJ.
Underwood, A., 1948. Fractional distillation of multicomponent mixtures.. Chem Eng Prog 44, 603–614.
Vatavuk, W.M., 2002. Updating the ce plant cost index: changing ways of building plants are reflected as this widely used index is brought into the 21st century. Chem. Eng. 109 (1).
Waltermann, T., Skiborowski, M., 2017. Conceptual design of highly integrated processes optimization of dividing wall columns. Chem. Ing. Tech. 89 (5), 562–581.